TECHNICAL MEMORANDUMS

NATIONAL ADVISORY COMMITTEE FOR AERONAUTICS

No. 558

MEASUREMENT OF PROFILE DRAG ON AN AIRPLANE IN FLIGHT BY THE MOMENTUM METHOD

By Martin Schrenk

PART II

From Luftfahrtforschung, May 18, 1928

Washington
March, 1930

NATIONAL ADVISORY COMMITTEE FOR AERONAUTICS.

TECHNICAL MEMORANDUM NO. 558.

MEASUREMENT OF PROFILE DRAG ON AN AIRPLANE IN FLIGHT BY THE MOMENTUM METHOD.*

By Martin Schrenk.

PART II.

V. Theoretical Considerations

a) Preliminary Remarks

The first practical requirement is to obtain reliable test results covering the various questions which arise in connection with constructional problems. Science endeavors to explain the technical side of these problems and to put the explanations into general numerical expressions which, according to their importance, are called hypotheses, theories or natural laws. Scientific progress is of course usually much more laborious and slow than is necessary to meet the immediate practical requirements of technical development. However, the knowledge gained from systematic scientific investigation eventually demonstrates its great practical value by providing a sound basis for further development instead of a confusing multitude of individual results.

The purpose of this section is to survey the present status of scientific knowledge of the causes which produce drag, in or-

*"Ueber Profilwiderstandmessung im Fluge nach dem Impulsverfahren" from Luftfahrtforschung, May 18, 1928; subsequently published in the 1929 Yearbook of the Deutsche Versuchsanstalt für Luftfahrt, pp.9-40. For Part I, see N.A.C.A. Technical Memorandum No. 557.

der, if possible, to establish the relation between the above-mentioned individual results and the actual phenomena which demonstrate the fundamental importance of surface conditions.

In a nonviscous flow the drag of a body is zero, provided it does not produce lift. Hence the drag actually produced is attributable to viscosity or internal friction.* However, very unsatisfactory results are obtained with simple equations for the determination of internal-friction drag by means of physical constants (viscosity and density). In fact, drag production is an extremely intricate process. It has been explained, however, during the past few years, by Prandtl and his assistants who, in developing the boundary-layer theory, have afforded a far-reaching insight into the mechanism of flow resistance, which consists of friction and "form drag." Both components are determined by the behavior of the boundary layer. Thus the maximum lift is also reduced to a small fraction of its theoretically possible value. The following statements are based on the publications by Prandtl, Von Karman, Hopf, and Schiller, as listed in the bibliography.

---

*Other causes may also create drag by separation of the flow, e.g., cavitation or the delivery of air to certain points from the inside of the body. In this connection, see "Ueber die Labilität der Potentialströmungen" by H. Föttinger, from Verhandlungen des zweiten internationalen Kongresses für technische Mechanik (Proceedings of the Second International Congress for Technical Mechanics, Zurich, 1926, pp.477 ff). In the present treatise, which deals exclusively with profile drag, these phenomena are negligible.

b) The Boundary Layer

Under all conditions of flow in confined fluids of slight viscosity (such as air and water under normal conditions), an extremely thin layer of the fluid adheres to the walls. From this layer, which has zero velocity, the flow velocity increases rapidly until it reaches the velocity of the free or potential flow. The whole layer, inside of which the velocity increases from zero to that of the free flow, Prandtl calls the "boundary layer."

Since the boundary layer is always very thin, it is assumed that there is no pressure drop in it perpendicular to the direction of flow. The static pressure of the boundary layer is determined rather by the pressure of the limiting potential flow. In the further treatment we will therefore distinguish between the regions of potential flow and the boundary layer.

The general course of the flow velocity in the boundary layer is shown in Figure 52. The flow in the boundary layer can be either laminar or turbulent. The former is a parallel displacement, while the latter is an irregular flow characterized by a main flow parallel to the wall and a superposed undulatory motion with components perpendicular to the wall.

When a flow encounters a body, the resulting boundary layer is at first very thin. Its thickness gradually increases in the direction of the flow, which is usually laminar at first. At a

certain point, however, it becomes turbulent. These conditions were investigated very thoroughly with tubes.

The transition of the flow from the laminar to the turbulent condition greatly depends on obstacles in front of the body, sharp edges, etc.* It also depends on the Reynolds Number already referred to in the introduction (velocity times the comparative length divided by the kinematic viscosity). There exists, however, a lower limit of the Reynolds Number ("critical" Reynolds Number) below which any disturbance fades away and the laminar boundary layer remains stable. It is interesting to note that this process takes place on smooth walls, i.e., in unilaterally bounded flow, at Reynolds Numbers of the same order of magnitude as those of tubes, provided the thickness of the boundary layer is substituted for the diameter of the tube in the calculation of these numbers. This reversion of the flow greatly affects the frictional drag.

c) Skin Friction

Skin friction is a result of viscosity and adhesion. Viscosity is the ability of a fluid to transmit shearing stresses. Unlike the corresponding phenomenon in solid bodies this transmission is not a static process, since the fluid has no definitely fixed shape. It depends on the difference between the veloc-

*Both cases refer to an exchange of momentum between two layers of different velocities. In laminar flow, the exchange takes place from molecule to molecule; in turbulent flow, from vortex to vortex.

ities of two adjacent fluid layers. In the case of uniform parallel flow, the shearing stresses are completely eliminated.

τ being the shearing stress and μ the viscosity coefficient, the following relation exists between these two factors (Fig. 53):

$$\tau = \mu \frac{dv}{dy} \; (= \mu \tan \varphi).$$

This expression is particularly important immediately on the boundary surface. No reference was made in the preceding section to the variation of the velocity in the immediate neighborhood of the wall. A definite conclusion can be reached on this subject by taking into consideration the fact that the whole frictional force exerted by the fluid must be actually transmitted to the wall by the immediately adjacent fluid layer in the form of shearing stresses. Since τ and μ are finite values, dv/dy must also have a finite value. Hence, by measuring this pressure drop immediately at the wall, the magnitude of the shearing stress exerted by the fluid on the wall can be determined for each point.

Such tests are now being made or have already been completed by certain laboratories. We refer, for instance, to the investigations in the laboratory of the Delft Technical High School (Reference 10)* where this value was determined by means of hot-wire instruments on a flat wall (glass plate). Figure 54 shows the variation of dv/dy and of the boundary-layer thickness δ

at a given velocity plotted against the extent of the plate. This shows that the shearing stresses are by no means the same at every point, but that after reaching a minimum, they rise considerably and then drop again. The flow changes from laminar to turbulent at the lowest point of the curve dv/dy. From this point the thickness of the boundary layer increases greatly. It is not the purpose of this report to go into further details, but only to show that the skin friction is not the same at all points and that it cannot generally be expressed by simple equations.

d) Form Drag

It has been shown that the boundary layer is very unfavorably affected by the pressure drop of the potential flow. So long as the pressure of the potential flow decreases along the wall in the direction of the flow, all goes smoothly, since the boundary layer then flows from high-pressure to low-pressure zones, thereby gaining energy. However, as soon as the point of minimum pressure is passed and the pressure of the potential flow begins to increase again, the boundary layer must, to a certain extent, flow up-hill. Owing to wall friction, the boundary layer has a tendency to slacken its pace and to expand, as was shown by the tests described above. Under the action of the increase in pressure, the motion is increasingly retarded, especially in the layers close to the wall. Finally the point is reached where, in the neighborhood of the wall, the velocity in

a layer of finite thickness becomes zero. From there on the motion in the neighborhood of the wall is reversed (Fig. 52). The boundary layer begins to separate from the wall and to penetrate the free flow, which carries it along in the shape of more or less regular vortices. The vortex trail is thus formed.

The result is a separation of the whole flow from the wall. From this point on, the actual direction of flow differs materially from that which would be theoretically anticipated. Since, under these conditions, the increase in pressure cannot take place correctly, negative pressure is created at the rear end of the body. The resultant of all the normal forces on the body which, in the case of potential flow, should theoretically be zero, is now given a finite value, the form drag, in the backward direction.

The process can also be represented as follows. The wing is a device designed to produce pressure perpendicular to the flow. This result is achieved by retarding the air below the wing and accelerating it above the wing. The kinetic energy of the accelerated air must be retrieved by a sort of diffusing action of the trailing edge of the wing. It is a generally known principle of hydrodynamics that diffusers, e.g., Venturi tubes, even of the best and slenderest type, do not fully convert kinetic energy into pressure. This fact is explained by the separation of the boundary layer.

e) Relation between Frictional and Form Drag

From the foregoing statements it is obvious that frictional and form drag cannot exist independently. The burble point of the flow is determined by the pressure distribution, as well as by friction phenomena. The form drag, however, depends largely on the position of the burble point. Behind this point, the shearing stresses decrease again to a small fraction of their value in the portion forward of the burble point. In other words, the frictional drag, in this case, is of only secondary importance. Hence, every variation of flow, which affects the separation, changes all the conditions of form and frictional drag. Slender bodies would have no form drag without frictional drag.

The most important result of this consideration is the fact that surface conditions not only directly affect the frictional drag, but also indirectly affect the form drag. Both are increased by rough surfaces.

f) Application to Profile-Drag Measurements

1. What, according to the present series of tests, is the relation between the form and the surface drag (skin friction) of thick wing sections? A satisfactory solution of this problem might be found by measuring either one of the two components by itself. This was done by Betz at the beginning of the war. He

found the form drag by measuring the pressure distribution over a Joukowsky section (Reference 11). The determination of frictional drag would require investigations regarding the course of dv/dy (according to Section V, c) to be made along the entire profile. The execution of such a test in flight would encounter considerable difficulties, principally due to the extremely small thickness of the boundary layer.

Hence we must at present confine ourselves to establishing a relation between our test results and the friction measurements on smooth surfaces. Fortunately, measurements are available with the same Reynolds Number and with the same relative length (t = 2 m) (Reference 3). The latter guarantees like relative roughness within reasonable limits (Section V, g). The comparison is made in Figure 55.* The variation in the Reynolds Number, caused by different flight velocities (lift coefficients) during the measurement of the polars, are likewise taken into consideration. The (dash) lines of friction measurements on smooth surfaces therefore bend to the left at the bottom. The conditions at an altitude of 2000 meters and 4°C were taken as the basis for the viscosity of the air. The departures from this mean value during the measurements are negligible.

The results agree surprisingly well with the friction measurements. The fact that the polars of smooth wings (flights 15,

*In order to obtain a reliable comparison of the measurements as regards frictional drag, the drag coefficients of the wing sections should be referred to the entire area of the wing portion under consideration instead of to double the plan area. The difference amounts to 4% for the wing section considered.

18, 31) are approximately parallel may lead to the conclusion that the profile drag consists chiefly of frictional drag, at least within the range of mean lift coefficients (from $c_a = 0.5$ to approximately 0.9), whence it is inferred that no appreciable separation has taken place. This assumption is confirmed by the observed course of the flow in the vortex trail which, for such smooth sections, is always very quiet. The rough wing 16 is in opposition to this. Its polar has no rectilinear portion. In this case, separation seems to take place at very small lift values. The same conclusion can be drawn from the greatly increased turbulence in the vortex trail and from its greater width. The fact that curve 16 has a friction which is partly inferior to that of flat surfaces of the same roughness is attributable to slightly different surface conditions.

A similar comparison was once made in Göttingen (Reference 3) between friction measurements on flat surfaces and profile-drag measurements about symmetrical wing sections. Even in this case with five to ten times smaller Reynolds Numbers, the profile-drag coefficients of moderately thick wings nearly reached the value of the friction coefficients of flat surfaces of the same nature.*

*The same problem is covered by British A.R.C. Reports and Memoranda No. 1015 (On the Drag of an Airfoil for Two Dimensional Flow, by A. Fage and L. J. Jones, 1925), which reached the author after the completion of his work. This report describes the measurements of pressure losses behind a thick wing section of 15 cm chord and their calculation according to a formula proposed by Taylor. The form drag is determined separately by pressure-distribution measurements. The report reaches the conclusion

(Continued at bottom of page 11)

The sum of the frictional and form drag of a wing section may sometimes be smaller than the pure frictional drag of a flat surface. Boundary-layer thickening always causes a reduction of the differential quotient dv/dy which determines the skin friction of the adhering layer (Section V, c). In the case of large linear dimensions and simultaneously large Reynolds Numbers, the increase in the form drag caused by the thickening of the boundary layer may well be more than offset by the reduction of the skin friction.*

2. The conditions of a corrugated sheet-metal wing (Fig. 45) will be considered briefly in this connection. Up to $c_a = 0.6$ the polars (flights 5+9 and 13) show more or less equal drag coefficients, but from there on they bend sharply to the right. As already mentioned, this can be attributed, from there on, to the noticeably different behavior of the flow on the upper and lower surfaces of the wing. As regards the lower portion of the polar, it is important to determine whether the flow

(Continuation of footnote on page 10)
that the smallest profile drag of this wing, for a mean section, consists of 80% form and 20% frictional drag, the latter being of the same order of magnitude as the (measured) frictional drag of a flat plate of like thickness at half the Reynolds Number. Owing to smaller Reynolds Numbers (R approx. 2×10^5) and to the reduced size of the models, the above results cannot be compared directly with the measurements in the present report. The relative roughness was probably rather great.

*This may be the reason why the superiority of thin wing sections with respect to drag, always apparent in model tests (for which reason racing airplanes are always provided with such wing sections) does not obtain in the same degree on full-size airplanes, as seems to be indicated by the results of this investigation. Hence the minimum drag seems to depend much more on surface conditions than on wing-section thickness.

conforms strictly to the corrugations of the sheet metal or whether dead angles form in the hollows.

A comparison was made with the tests of the smooth profile painted with aluminum-bronze the same as the corrugated sheet metal (flight 33 - Part I). Unfortunately it did not afford a good basis for comparison, owing to its S-shaped curve. $C_W = 0.75$ can be assumed to be the mean drag coefficient in the region considered, as against $C_W = 1.10$ for corrugated sheet metal. If only surface drag is produced in both cases, the relation between the two drag coefficients is approximately the same as that between the corresponding surfaces. According to the results obtained with the tested wing portion, the ratio between the surfaces of the corrugated and of the smooth sheet metal was found to be 1.15. Hence the drag coefficient of the corrugated sheet metal would be $0.75 \times 1.15 = 0.86$. The fact that it is actually much greater shows that the conditions are not so simple.

This is probably due largely to the rivets which secure the sheet to the spars at the bottom of each corrugation. Taking measurement 23 (smooth sheet metal with rivet heads and a coating of aluminum bronze) as the basis of comparison, in which C_W = approx. 1, there is practical agreement with the corrugated sheet-metal measurements. No definite conclusions should be made, however, since the effect of small obstacles still requires very thorough investigation.

g) Different Kinds of Roughness

Considering the physical processes in the boundary layer, as outlined above, it is obvious that the thickness of the boundary layer and the roughness of the surface must stand in a certain relation to each other as regards their effect on the drag. If the unevennesses are small in comparison with the thickness of the boundary layer, they cannot disturb the flow as much as unevennesses several times the thickness of the boundary layer.

Investigations made with tubes show that a "relative roughness" can be spoken of, if it is understood to mean the ratio between the individual surface elevations and a relative dimension of the tube (e.g., the diameter). The behavior of tubes having the same relative roughness is the same under the action of drag, provided all the other conditions (same Reynolds Number) remain unchanged.

Measurements by Hopf and Fromm (References 7 and 8) seem to require a distinction to be made between two different kinds of roughness. One is the actual roughness caused by very small sharp-edged obstacles (file-like surface). The drag coefficient of such a surface is independent of the Reynolds Number. The other kind of surface condition can be called "corrugated." It consists of more or less gentle elevations of larger dimensions. Its drag coefficient, like that of smooth surfaces, follows an exponential law as a function of R. Between these two kinds

of roughness there is an infinity of degrees. Both kinds of roughness were measured during the present tests. The results, however, do not disclose any characteristic distinction, since no variation of the Reynolds Number was possible except that which automatically recurred during every flight.

Attention is also called to the fact that, beyond a certain degree of surface smoothness, it seems impossible to achieve any further reduction in the flow resistance. This "absolute smoothness" seems to be that of glass and polished metal surfaces. During the present investigations this state seems to have been very closely approached by smooth sheet duralumin. Any further reduction in the profile drag of thick wing sections is therefore hardly to be expected.

h) High-Pressure Wind-Tunnel Tests

In order to make wing-model tests with Reynolds Numbers similar to those of actual flight and thus facilitate the subsequent conversion of the test results, it is now the practice in America to place the wind tunnel in a high-pressure chamber with an over-pressure of about 20 atmospheres. Thus, for equal flow velocity, the value of the Reynolds Number is approximately doubled. Tests were made in this tunnel with wing models having an aspect ratio of 6 : 1 up to Reynolds Numbers of 3.5×10^6.

The conversion of such test results to full-size conditions does not, however, fully meet the requirements of the law of

similarity, since the latter states that the geometric similarity of the compared bodies must be the basis of their hydrodynamic similarity. During these tests the 12.7 cm chord of the tested wing models (Reference 12) was so much smaller than that of the actual wing that even a polished surface would seem rather rough, if its size were similarly increased.

In fact, a comparison of atmospheric wind-tunnel measurements with those of the present work proves that this statement is at least qualitatively correct. The Göttingen wing section 387 was used. This is quite similar to the tested Junkers wing section, but has a somewhat smaller camber ratio (thickness = 0.15 x chord). The comparison in Figure 56 shows that the relative roughness of the small model is similar to that of the wing of 2.1 m chord, covered with a layer of twice-doped fabric.* Yet, by forming a difference, the profile drag of the small model was derived from a test of the actual wing. The possible error cannot, however, be so large as greatly to affect the comparison in favor of the small model.

i) Roughness and Maximum Lift

A very important point in aeronautics remains to be considered. The above-mentioned separation phenomena cause the flow to leave the upper surface of the wing before it reaches the

*It is assumed that the deviation of polar 387 from its regular course at mean lift coefficients is due to some disturbance outside of the model.

trailing edge. Between the two flow regions, on the upper and lower sides of the wing, there is formed at the trailing edge a dead-air wedge, the boundary surface of which, beginning at the burble point, practically assumes the function of the profile surface and bounds the potential flow. The total deflection of the flow is thereby somewhat reduced, since the trailing angle of this "apparent profile" is smaller than that of the original wing section. Since, on the other hand, the lift is directly produced by this deflection of the flow, its reduction causes a decrease in the lift.

The above-mentioned work by Betz (Reference 11) contains a good confirmation of this statement as calculated from pressure-distribution measurements about the wing section. A further confirmation is found in the measurements made by Wieselsberger on a profile with different surface conditions (Reference 13). The result is given in Figure 57, where points of equal angle of attack are connected by oblique lines. The different degree of sensitivity of individual portions of the wing section to the influence of roughness was tested by Oskar Schrenk (Reference 14). Roughness of the upper wing surface near the leading edge has a particularly disturbing effect, owing to the fact that the boundary layer is very thin at that point. The maximum lift is also greatly reduced by roughness since, regardless of the degree of roughness, the flow always separates at about the same angle of attack.

A comparison of Figure 57 with Figure 46 or 47 immediately shows the conspicuous qualitative agreement of the two values. All drag coefficients of the actual wing are much smaller (as is also the relative roughness), but there is a good agreement in the character of the curves and in the strong increase of the profile drag of rough wings from small lift coefficients upward. Moreover, the increasing roughness of a profile reduces the angle of attack at which turbulence begins in the vortical region. This is confirmed by the first diagrams of the results, as plotted in Figures 12 to 24. Hence, it was often impossible to make accurate measurements at large lift values.

It is consequently established that surface roughness and the form in which it actually manifests itself considerably affect the lift as a function of the angle of attack and particularly the maximum lift. This could not have been proved directly by the momentum method without pressure-distribution measurements.

VI. Conclusions and Prospects

a) Practical Significance of the Results

1. A numerical demonstration of the influence exerted by the profile drag on airplane performances would exceed the limits of this report. These conditions are only briefly outlined, it being assumed that the method of performance calculation is generally known.

There are two fundamentally different kinds of airplane drag. One kind is closely related to the process of lift production. It originates in the irrecoverable kinetic energy of the downwash and is called the induced drag, on account of its mathematical analogy with certain processes in electrodynamics. The other kind is due to friction and incomplete conformation of the flow to the different parts of the airplane. It is called head resistance, since the air forces act only in the opposite direction to that of the flow. It also includes the profile drag, that portion of the wing drag which is independent of the lift production and depends only on the surface conditions of the wing.

Head resistance plays only a subordinate role in climbing flight (Reference 15), but its influence is decisive in level flight. In the performance equation of level flight, head resistance has the same value as the engine power, at least for normal power loadings (lb./hp) at moderate altitudes. Thus, at a given speed, any reduction in the head resistance has the same effect as a corresponding increase in the engine power. It is even more effective than the latter, since any increase in the size of the engine causes an increase in the head-resistance area, a reduction in the propeller efficiency and an increase in the weight of the airplane.

The profile-drag component of the head resistance increases with increasing dimensions of the aircraft, since on the one hand, the fuselage, engine nacelles, and other airplane parts

are gradually absorbed by the wing while, on the other hand, the available useful space does not generally increase quite as the 3/2 power of the wing area. For the ideal case of "flying wing," the head resistance would consist of the profile drag only. When it is remembered that all airplane parts are similarly affected by surface roughness, its importance is very manifest, even for airplanes of ordinary size.

2. The effect of surface conditions on the maximum lift, as confirmed by the present tests, is very important for the reduction of the landing speed. The remarkable differences between the landing speeds of airplanes identically loaded and having similar wing sections is often due to this fact.

3. Smooth and undisturbed wing surfaces cause an increase in the maximum speed and a reduction in the landing speed. Such improvements, achieved by comparatively small efforts, often materially increase the speed range of airplanes and consequently the economy and safety of flying.

4. The tested wing sections had a ratio of maximum thickness to chord between 1 : 5 and 1 : 6. Plywood covering I had a ratio of nearly 1 : 5. In the interest of economical flight this ratio has been hitherto regarded by designers as the limit. According to the present results, however, even thicker wing section may give useful aerodynamic values, provided they are smooth enough. The importance of thick wing sections is obvious for the construction of cantilever wings of large aspect

ratio (torsional rigidity, covering to resist part of the bending stress, stowing of cargo).

b) Regarding the Continuation of the Tests

From what has been said, it is obvious that this method stands at the very beginning of its development and may still bring many surprises. A short outline is given below, on the basis of the experience gained, to indicate the direction further investigations may take.

1. First, a number of problems may still be solved with the existing installation. The purpose of the experiments would be, on the one hand, to gain further experience with this method and, on the other hand, to solve a series of theoretically and practically important questions. The following tests are suggested, but they do not, of course, exhaust all the possibilities:

Varying the distance of the rear static tubes from the wing;

Tests at the trailing edge of the wing, for the separate determination of the effect of the upper and lower surfaces of the wing;

Measurements behind different cross sections, especially behind the ailerons;

Investigations with static tubes of different sizes and types capable of better recording the delicate structure of the vortex trail;

Momentum measurements with sensitive static tubes at different points of the upper surface of the wing for determining the cause of discontinuities and separation;

Testing methods for artificially damping the vibrations of the alcohol columns by reducing the diameter of the U-tubes, in order to diminish the scattering of the points.

2. The investigations suggested under a, 4, to be made with other and especially with thicker wing sections, may, of course, if not otherwise feasible, be made with the aid of superstructures mounted on the wings of the airplane hitherto used. This method was explained by the writer in his lecture before the W.G.L. In order to produce a more or less regular flow, the wing portions with different profiles would have to be provided with end disks. The lift coefficients of these wing portions would then no longer equal the lift coefficient of the whole wing and would have to be determined separately by pressure-distribution measurements. However, it would be difficult to operate such an installation and impossible to include all desired angles of attack. A better solution of the problem is therefore given below.

3. The wing section to be tested is not mounted on the airplane wing, but is mounted in a movable and independent way as a large-sized model. On a large airplane of the size of the Junkers G 24, wings with a chord of 2 to 3 meters can be safely mounted above the center of gravity without materially impairing the flight characteristics.

The total pressure measurement is made (according to Betz) by means of a set of static tubes which indicate simultaneously all the total pressures on a single instrument board. The static pressures are measured separately. They need to be measured at only a few points since their variation and effect are small.

The measuring board and camera are located in the cabin where they are protected from the air flow. The adjustment of the wing and measuring gauges is controlled from the cabin. The pressures at the perforations of the wing are indicated and simultaneously photographed on the board. They are used for calculating the lift and moment coefficients. This arrangement affords great freedom in the choice of the angles to be measured and enables quick work. A test flight, for the determination of a polar with all three components, did not require more than 15 minutes in good weather, including the take-off and landing. This arrangement also enables the measurement of a series of Reynolds Numbers with the same model at different flight speeds. Furthermore, the simultaneous measurement of all the pressures may enable important conclusions regarding the flow phenomena.

The correctness of the results may be impaired by a curvature of the flow due to the circulation about the main wing. It was found by calculation, however, that the resulting error cannot be large. Nevertheless, the field in which the model wing was to be measured had to be carefully investigated by preliminary tests with a static tube and a flow-direction indicator

(e.g., a cylinder with three perforations). These investigations were also intended to include the effect of the fuselage and propeller slipstream. If the circulation about the main wing should cause a noticeable bending of the flow, measurements might, for instance, be made with certain wing sections placed in an inverted position, thus offsetting the errors caused by the bend. The most suitable aspect ratio of the model wing also had to be determined by preliminary wind-tunnel investigations, both as regards the effect of the edges on the point of measurement (wing center) and on the cost of the model which forms a large part of the total expense.

The profile drag and the maximum lift of practically all existing wing sections can be determined by means of this installation, some of the most important questions being the characteristics of the thickest and thinnest wing sections, the maximum lift of symmetrical wing sections, and the effect of different cambers. This program would require some 30 models carefully selected from the best-known shapes. Moreover, this would enable the investigation of certain special problems which cannot be satisfactorily solved in the air stream on account of the Reynolds Numbers; for example, the problem of the slotted wing or the removal of the boundary layer by suction.

VII. Summary

The theoretical bases of the momentum method are first presented, and the corresponding equations are developed. The quite unusual method of measurement is described in detail. In this connection particular attention is called to the accuracy of measurement.

The author then describes measurements made by him with a two-seated Junkers airplane. 24 polars of a thick wing section with different wing coverings were obtained by flight tests. Tests were made with Junkers corrugated sheet metal, plywood and fabric with different degrees of doping, artificially roughened with poppy seed; also two different kinds of sheet metal, plain and varnished, with and without rivets. The results are represented by polars and their reliability is discussed. It is shown that the profile-drag coefficients are surprisingly affected by surface conditions. The coefficients obtained for smooth surfaces are considerably smaller than the results of wind-tunnel tests with similar wing sections.

Another section deals with the essential features of Prandtl's boundary-layer theory, as developed during recent years, and with the explanation of profile drag, as derived from this theory. It is endeavored to establish a relation between these theories and a few special phenomena observed during the tests. This is achieved by comparing the profile-drag measurements with

friction measurements on flat plates and by studying the relation between maximum lift and roughness. Lastly, the practical importance of the results is discussed and suggestions are made regarding further investigations.

A p p e n d i x

Suggestions for Simplifying the Calculation

1. In the first place, the equation used can be simplified so as to greatly reduce the work of calculation. A further step is taken by considering the numerical influence of the second integral. When the static pressure in the vortex trail is assumed to be constant and the total pressure loop is given a mean value, the second integral can be expressed in fractions of the first integral as a function of the static pressure and of the maximum value of the total pressure. Under these simplifying assumptions, which do not differ materially from the actual conditions, the work can be confined to the determination of the total pressure loop and of the mean static pressure in the vortex trail, from which, by a short calculation, the drag coefficient can be derived with sufficient accuracy.

2. After introducing the dynamic pressures, equation (7a) can also be written as follows:

$$W = l \int (g_o - g)\, dy + l \int (q_i - q)\, dy - 2l \int \sqrt{q_\infty}(\sqrt{q_i} - \sqrt{q})\, dy \qquad (7b)$$

According to Section II, c, 6 (Part I)

$$q_i - q = g_o - g.$$

Thus equation (7b) becomes

$$W = 2\,l \left\{ \int (g_o - g)\,dy - \int \sqrt{q_\infty}\,(\sqrt{q_i} - \sqrt{q})\,dy \right\} \qquad (11)$$

This equation greatly simplifies the numerical calculations which are the necessary preliminary steps toward the solution.

5. We shall now turn our attention to the second integral of equation (8). Considering that, according to Section II and Figure 3,

$$q_i = q_\infty - p$$

$$q = q_\infty - p - (g_o - g)$$

it is obvious that the value of the integrand depends on the two values p and $(g_o - g)$. Thus, when $(g_o - g)$ and p are known at a point y, the second integrand at the dynamic pressure q_∞ can be calculated for this point. The result of such a calculation, in which $(g_o - g)$ and p vary within a practically important region, is represented by Figure 58. The abbreviation $\Delta (g_o - g)$ was adopted for the integrand with the intention of expressing the second integral as a fraction of the first integral. Equation (8) would then read

$$c_w = \frac{1}{t\,q_\infty} \left\{ \int (g_o - g)\,dy + \int \Delta\,(g_o - g)\,dy \right\} \qquad (8a)$$

In Figure 59 a ratio was established between the second integrand $\Delta (g_o - g)$ and the first integrand $(g_o - g)$.* This ratio is found to increase as the expression for the total pressure difference $(g_o - g)$. In order to obtain a definite value for the whole second integral, two assumptions must be made. The first assumption refers to the static pressure, which is considered constant throughout the whole turbulent zone. The second deals with the course of the total pressure difference $(g_o - g)$, the magnitude of which affects, as stated above, the value of the second integral at every point. Three cases were investigated in this connection. In addition to a mean ("normal") loop shape, as obtained by measurements, there were also assumed a rectangle for the upper and an isosceles triangle for the lower limit, both having the same area and altitude. The conditions of the normal loop are represented by Figure 60. The difference areas between the $(g_o - g)$ curve and the curves p = constant represent the values of the second integral, and hence the total result is represented by the areas below the curves p = constant. Integration can now be proceeded with.

After making these calculations, it only remains to determine the maximum total-pressure difference and the static pressure. Thereupon the part of the second integral in the first integral can be directly determined regardless of the influence of the shape of the total pressure loop. The result is shown in Figure 61. The values of the normal and of the triangular

*The lines of this figure are not perfectly straight, but are nearly so within the chosen range.

loop agree so well, that they were not plotted separately. The rectangular loop, however, differs materially.* Nevertheless, it is extremely improbable that the total pressure loops will ever approach the shape of a rectangle. Under ordinary conditions the values of the normal loop may be considered sufficiently accurate.

Figure 61 affords a very practical basis for simplifying the drag measurements by the momentum method. If the test point is located sufficiently far from the trailing edge of the wing, it may be assumed that the static pressure in the turbulent zone can generally be approximately expressed by a straight line, whereby the pressures in the middle of the vortex trail require more attention than those near the edge. In this case the static pressure needs to be determined at only two or three points. The value of the second integral can then be obtained directly from Figure 61, after plotting and integrating the $(g_o - g)$ loop.

Perhaps we may go a step farther. The static pressure behind the wing is affected, in the first place, by the circulation and by the distance of the point of measurement from the wing. The effect of the vortex trail is another item concerning which no accurate information is yet available. When this influence is practically independent of surface conditions and of the shape of the wing section or when its relation is accurately

*The lines are the same as in Figure 59, since $(g_o - g)$ is constant in this case.

known, it only remains to measure the total pressure difference behind the wing. The static pressure difference is then derived from a diagram as a function of the lift coefficient, from the relative distance of the static tube and perhaps also from the wing-section influences.

Owing to the fact that the evaluation of the momentum measurements still necessitates a rather extensive numerical calculation, the above-indicated simplification would materially reduce the cost and greatly facilitate the application of the momentum method of measurement.

Translation by
National Advisory Committee
for Aeronautics.

References

1. Betz, A. : "Ein Verfahren zur direkten Ermittelung des Profilwiderstands," Zeitschrift für Flugtechnik und Motorluftschiffahrt, 1925. (T.M. No. 337: A Method for the Direct Determination of Wing-Section Drag.)

2. Weidinger, H. : "Profilwiderstandsmessungen im Fluge," 1926 Yearbook of the Wissenschaftliche Gesellachaft für Luftfahrt.

3. Prandtl, L. : Ergebnisse der Aerodynamischen Versuchsanstalt zu Göttingen, Reports I and II, 1923.

4. Kumbruch, H. : "Messung strömender Luft mittels Staugeraten," Forschungsheft No. 240 des Vereines deutscher Ingenieure.

5. Prandtl, L. : "Ueber Flussigkeitsbewegung bei sehr kleiner Reibung," Vier Abhandlungen zur Hydrodynamik und Aerodynamik. (T.M. No. 452: Motions of Fluids with Very Little Viscosity.)

6. Von Karman, : "Ueber die Oberflächenreibung von Flussigkeiten," Vorträge aus dem Gebiet der Hydro- und Aerodynamik (Innsbruck 1922), Berlin 1924, p.125.

7. Hopf, L. : "Die Messung der hydraulischen Rauhigkeit," Zeitschrift für angewandte Mathematik und Mechanik, 1923, p.329.

8. Fromm, : "Stromungswiderstand in rauhen Rohren." Zeitschrift für angewandte Mathematik und Mechanik, 1923, p.339.

9. Schiller, : "Experimentelle Untersuchungen zum Turbulenzproblem," Zeitschrift für angewandte Mathematik und Mechanik, 1921, p.436.

10. Van der Hegge-Zijnen, B. G. : "Measurements of the Velocity Distribution in the Boundary Layer along a Plane Surface," Mededeeling 6 uit het laboratorium voor Aerodynamica en Hydrodynamica der Technische Hoogeschool Delft, 1924.

11. Betz, A. : "Untersuchung einer Schukowsky-Tragfläche," Zeitschrift fur Flugtechnik und Motorluftschiffahrt, 1915, p.173.

12. Munk, Max M. and Miller, Elton W. : "The Aerodynamic Characteristics of Seven Frequently Used Wing Sections at Full Reynolds Number." (N.A.C.A. Technical Report No. 233, 1926.)

13. Wieselsberger, C. : "Die wichtigsten Ergebnisse der Tragflugtheorie und ihre Nachprufung durch den Versuch," Vorträge aus dem Gebiet der Hydro- und Aerodynamik (Innsbruck 1922). Berlin, 1924, p.47.

14. Schrenk, Oskar : "Oberflächenrauhigkeit auf Tragflügeln," Vorlaufige Mitteilungen der Aerodynamischen Versuchsanstalt Gottingen, No. 4.

15. Schrenk, Martin : "Zur Berechnung von Flugleistungen ohne Zuhilfenahme der Polare," Zeitschrift fur Flugtechnik und Motorluftschiffahrt, 1927, No. 7; also published in 1927 Yearbook of the Deutsche Versuchsanstalt für Luftfahrt. (T.M. No. 456: Calculation of Airplane Performances without the Aid of Polar Diagrams.)

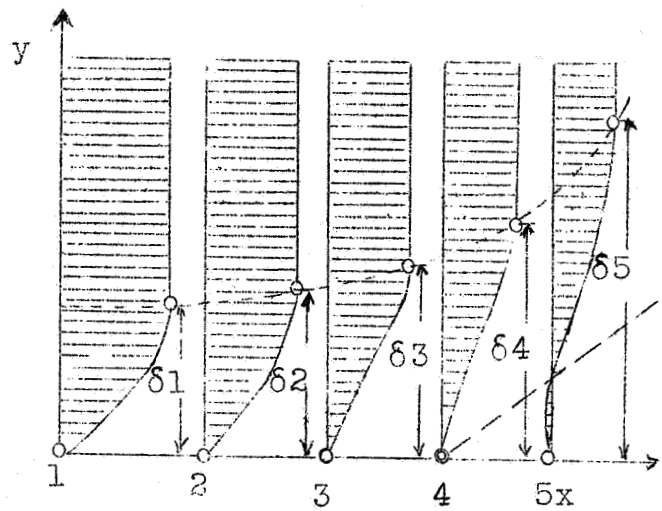

Fig.52. Velocity at different points on the surface of a body. x is the length of the body in the direction of flow. The separation of the boundary layer begins at 4. The ordinates are greatly magnified in comparison with the abscissas.

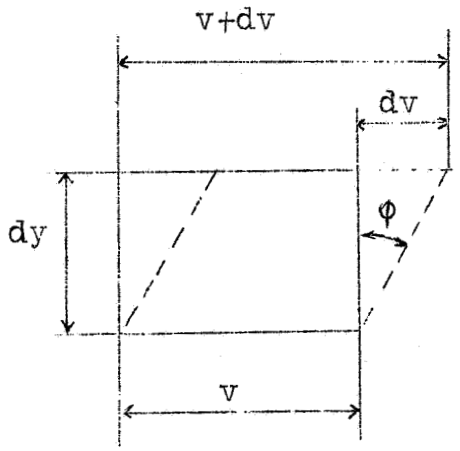

Fig.53. For definition of shearing stress in viscous fluids.

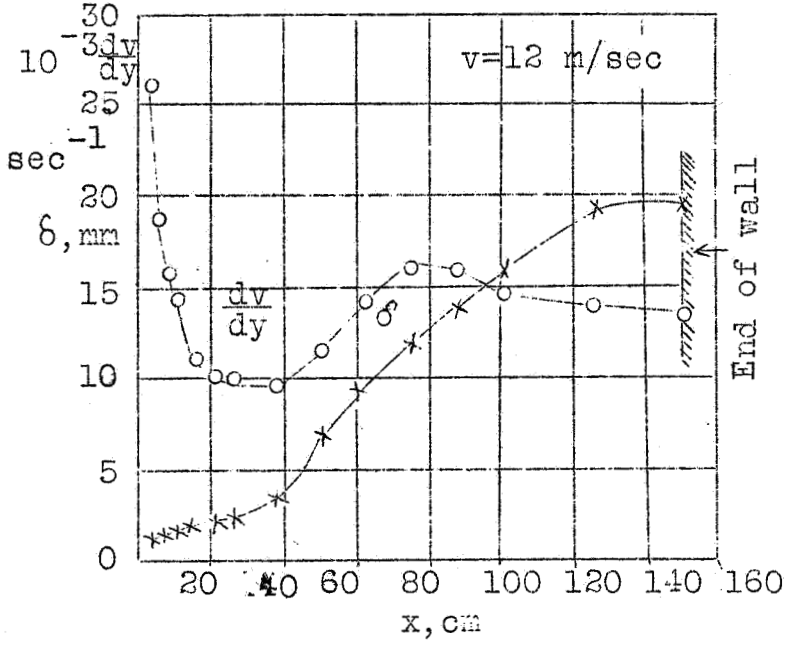

Fig.54 Velocity drop $\frac{dv}{dy}$ in immediate neighborhood of wall and boundary-layer thickness δ on a flat plate. (From the Durch report listed No. 10 in bibliography).

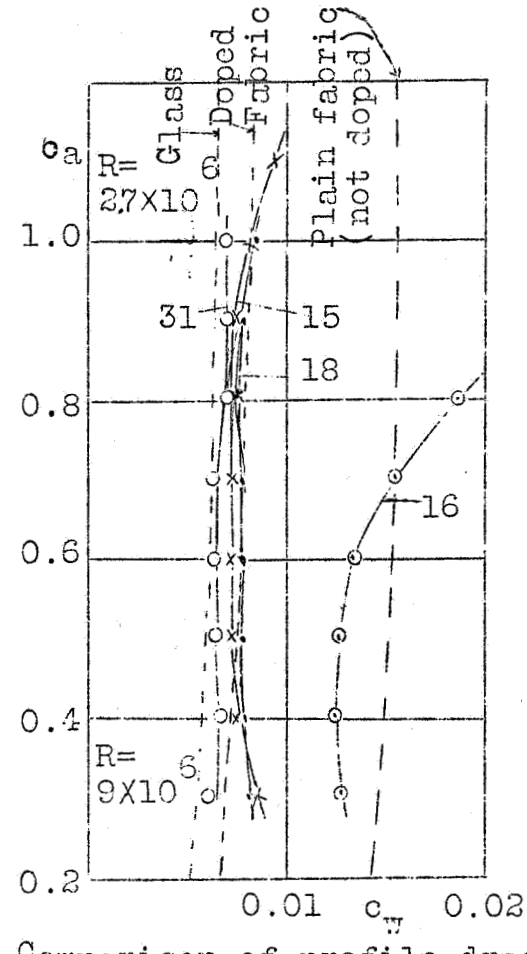

Fig.55 Comparison of profile-drag measurements with friction measurements on flat surfaces. Flight 31, 0.9 mm sheet duralumin, rivet heads removed, smooth. Flight 15, plywood covering II varnished and polished. Flight 18, plywood covering II with fabric 6 times doped and polished. Flight 16, plywood covering II with coarse fabric not doped.

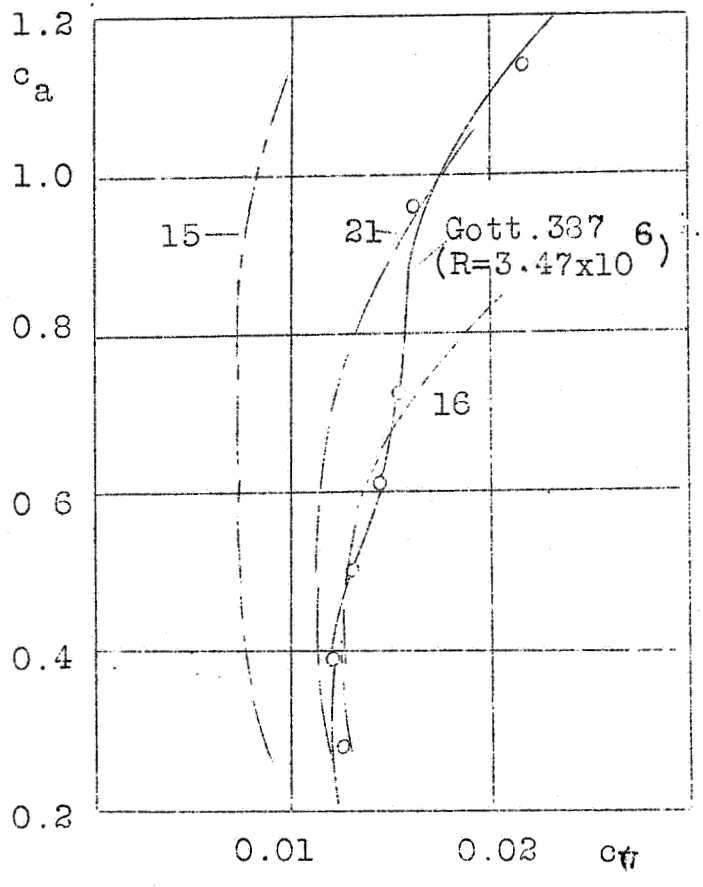

Fig.56 Comparison of a profile measurement in high-pressure wind tunnel (plain line) with measurements at the same Reynolds Number in actual flight.
15 plywood varnished and polished.
21 fabric twice doped and slightly polished.
16 fabric not doped.

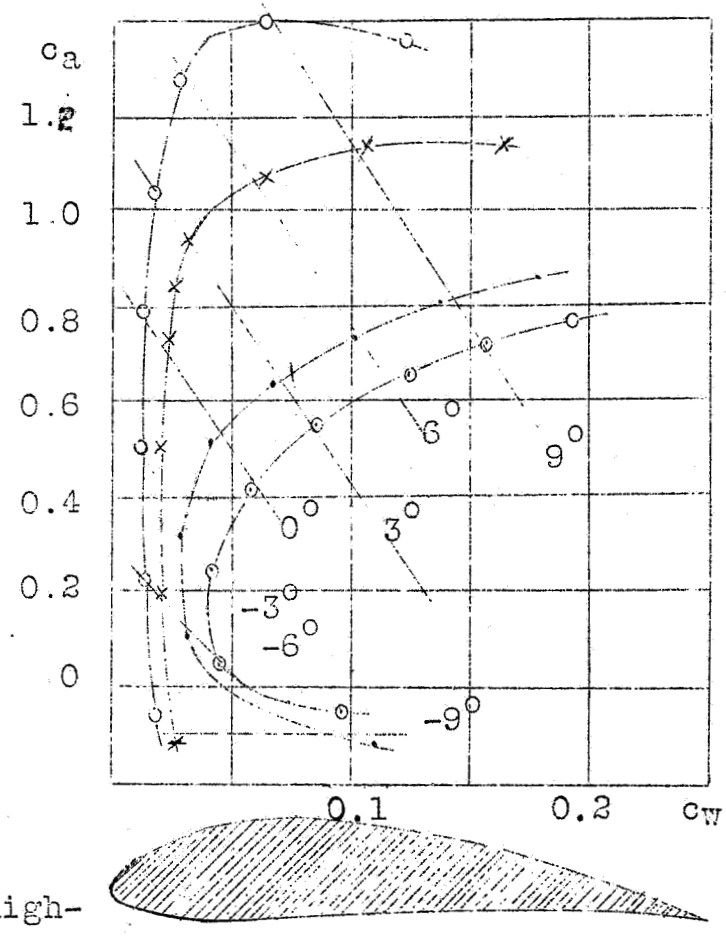

Fig.57 Roughness and maximum lift of model.

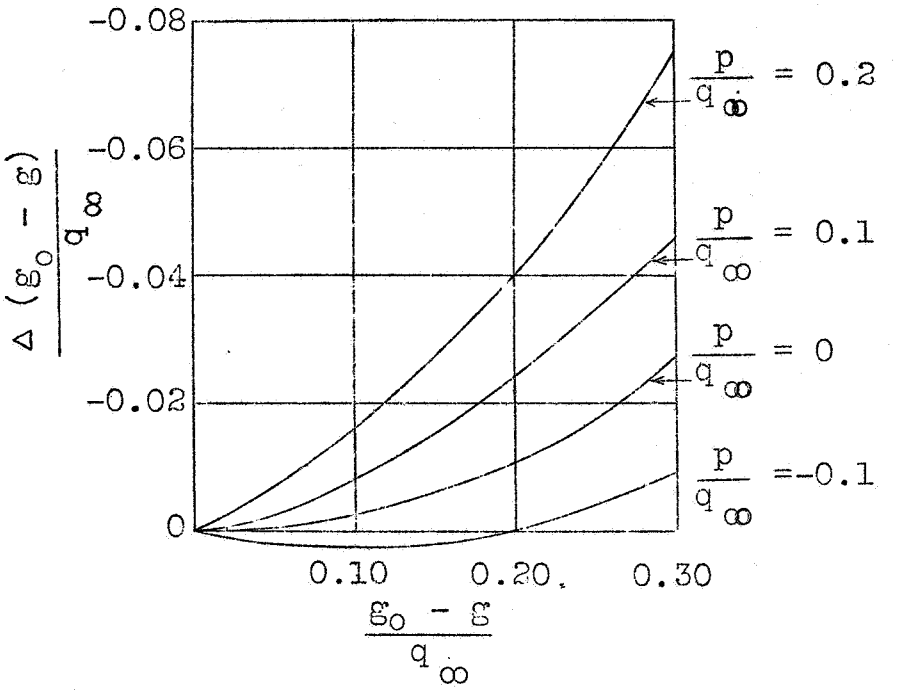

Fig.58 Absolute value of second integrand in Betz's equation plotted against total pressure and static pressure.

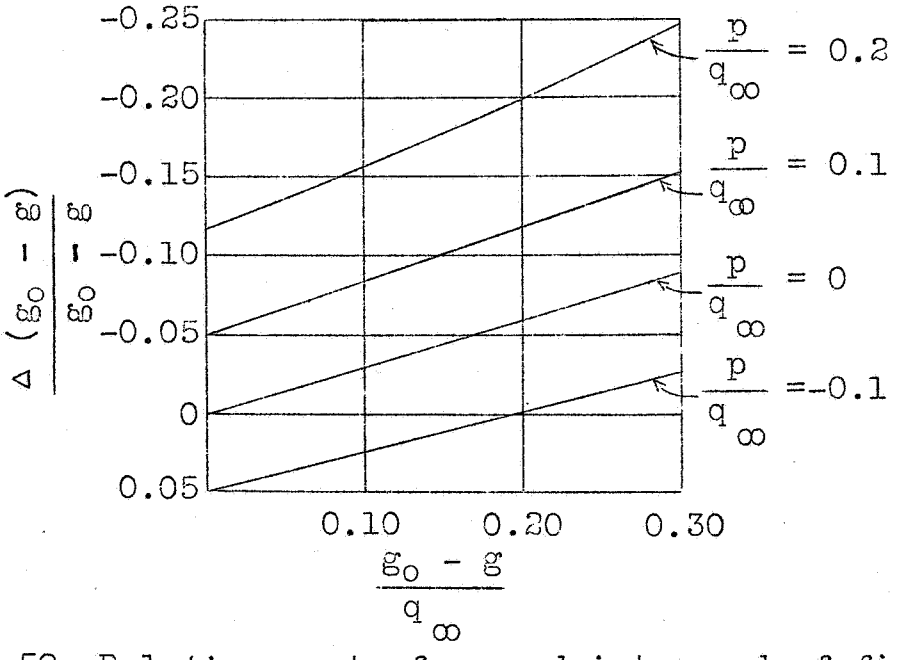

Fig.59 Relative part of second integrand of first integrand of Betz's equation plotted against total pressure and static pressure.

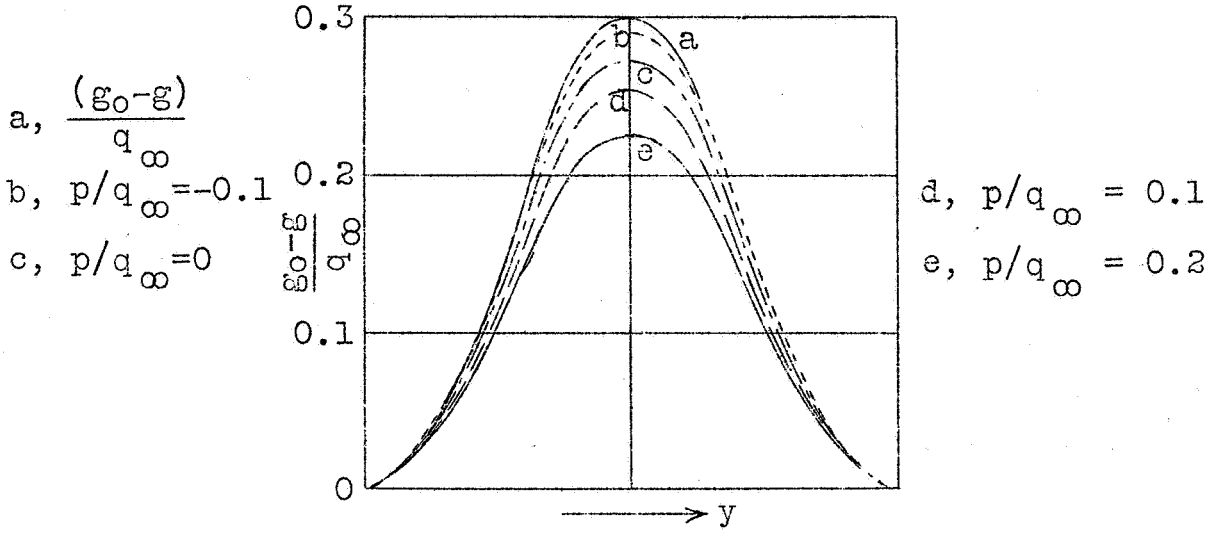

Fig.60 Effect of second integral on result at p = const., the maximum ordinate for the normal total pressure loop being 0.3 q_∞.

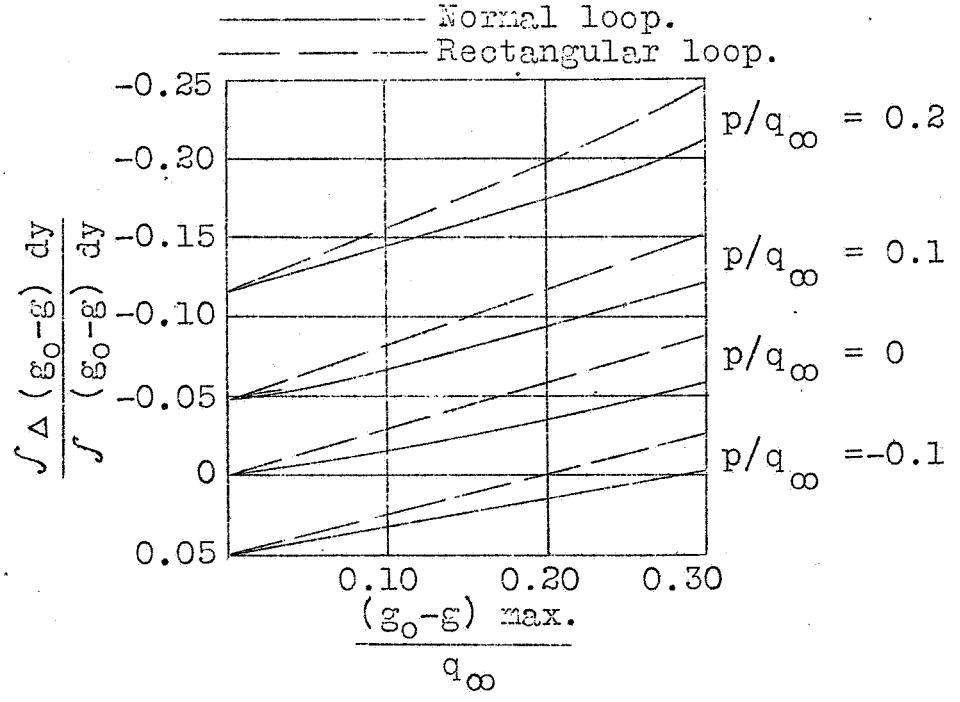

Fig.61 Ratio of second to first integral for normal (approximately triangular) and rectangular loops, plotted against maximum total pressure drop and static pressure.